Pergamon

Int. J. Mach. Tools Manufact. Vol. 38, No. 3, pp. 177–195, 1998

Printed in Great Britain
0890–6955/98$19.00 + .00

PII: S0890–6955(97)00040-0

TOOL PATH GENERATION FOR NC GRINDING

R. SARMA† and D. DUTTA‡§

(*Received* 25 *November* 1996; *in final form* 9 *May* 1997)

Abstract—A new method for tool path generation for grinding is proposed. This method for tool path generation is based on a conceptually simple yet fundamental representation of the manufactured surface. Such representations of the manufactured surface, which are derived analytically, were traditionally derived by measurement based methods. The representation of the manufactured surface is also advantageous in developing analytical estimates of surface roughness. These analytical estimates provide a starting point for the measurement or inspection operations which are usually data intensive and often times expensive for free-form surfaces. This paper thus presents an integrated approach to tool path generation which takes into account the manufacturing and measurement activities. © 1998 Elsevier Science Ltd

1. INTRODUCTION

The fabrication of dies and molds (typically used in the automotive, aerospace, ship building and health care industries) is a time consuming process. It has been documented [1] that the total time for producing a die or mold, from the design to the inspection, varies from 1200 to 3800 h. The largest amount of time (35–50%) is spent in finishing the die or mold. This paper proposes techniques capable of reducing the time spent in finishing dies and molds.

Some of the process plans for manufacturing dies and molds are summarized in Table 1 from Lange [2]. The most common process plan, for manufacturing large and geometrically complex dies and molds, involves using a near net shape process such as casting or forging followed by various finishing operations, e.g. milling, grinding, electro-discharge machining (EDM), electro-chemical machining (ECM), polishing, etc.

Numerically controlled (NC) machining (milling and grinding) may be used either directly or indirectly in all the above mentioned finishing operations. NC machining, followed by grinding and polishing, may be used directly to finish the dies and molds. NC machining may be used indirectly to manufacture the electrodes required for EDM and ECM. While NC machines have provided the die and mold industry with an efficient (quick and accurate) method to manufacture complex surfaces, this efficiency is realized

Table 1. Comparison of different plans for die manufacturing

Plan	Roughing	Pre-finishing	Finishing	Advantages	Disadvantages	Automation
1	Machining	Machining	Grinding/polishing	Fast	Finishing mostly manual	Medium
2	Machining	Machining	EDM	Accurate	Extra setup required	High
3	EDM	—	EDM	Accurate	Slow	High
4	Casting	—	Grinding/EDM	Near net shape obtained	Slow	Low
5	—	—	ECM	Fast and accurate	Complex electrodes required	High

†Department of Mechanical Engineering, Iowa State University, Ames, IA S0011, U.S.A.
‡Department of Mechanical Engineering and Applied Mechanics, The University of Michigan, Ann Arbor, MI 48109, U.S.A.
§Author to whom correspondence should be addressed

only when the coded instructions to the machine are efficient. Hence, the generation of coded instructions or *manufacturing data generation* for machining is an important step in efficiently manufacturing dies and molds.

This paper is focused on developing efficient methods of manufacturing data generation for NC grinding of dies and molds made of free-form surfaces. A significant part of the manufacturing data generation involves *tool path generation*. Specifically, a new technique for tool path generation that maximizes the material removal along the tool path will be developed for grinding. This new technique for tool path generation for grinding is enabled by a conceptually simple yet fundamental representation for the excess material left behind after the milling process.

Henceforth, the nominal die or mold surface will be referred to as the *nominal surface*. The *workpiece* or *milled surface* refers to the unfinished die or mold, and the *manufactured surface* refers to the finished die or mold. The rest of this section is structured as follows. Section 1.1 describes the background on free-form surface grinding and is followed by Section 1.2 which contains a literature survey.

1.1. *Background on NC grinding*

Grinding is the collective name for machining processes which utilize hard abrasive particles as the cutting medium [3]. In this paper it is assumed that the grinding operation is performed on a workpiece after it is milled on an NC milling machine. The different types of NC grinding machines available in the market and the types of grinding tools available are outlined in this section.

There are two groups of grinding machines which are used in free form surface grinding [4], (a) machine tool group and (b) articulated robots group. The advantage of grinding machines in the machine tool group* is that they are rigid compared to the ones in the articulated robot group. The advantage of grinding machines in the articulated robots group† is that they are versatile in positioning compared to the ones in the machine tool group. Both types of grinding machines can be used with two types of grinding wheels which are discussed below.

The grinding wheels that are used in material removal can be either rigid or flexible [5]. The advantage of using rigid grinding wheels is that their size and shape is known, and hence the positioning of the grinding wheel relative to the nominal surface is easy. In addition, high material removal rates can be achieved. The disadvantage faced by rigid grinding wheels is that their size depends on the largest curvature of the nominal surface, and this usually results in small grinding wheels making it difficult to achieve the high surface speeds required for grinding. Flexible grinding wheels are attractive due to their capability to conform to the shape of the nominal surface. However, the depth of cut cannot be accurately specified and hence the shape of the manufactured surface needs to be controlled indirectly.

The grinding wheels of interest in this paper are referred to as mounted abrasive wheels, specifically the ball-shaped mounted abrasive wheels, which are frequently used for finishing parts made of free-form surfaces. These mounted abrasive wheels are available in several shapes and sizes [6]. Conventional abrasive particles used on such wheels are aluminum oxide and silicon carbide. The abrasive particle size is specified in terms of the grit size, which is related to the sieve size used for sorting the abrasive particles [3].

1.2. *Literature survey*

The literature survey in the field of grinding can be divided into three groups: (a) NC grinding machines; (b) manufacturing data generation for grinding; and (c) process models and process control for grinding. The types of NC grinding machines have been summar-

---

*Companies that manufacture grinding machines of the machine tool group include Junker and Hitachi-Seikei.
†Companies that manufacture grinding machines of the articulated robot group include Aida Engineering Ltd and Showa-Seiki Ltd.

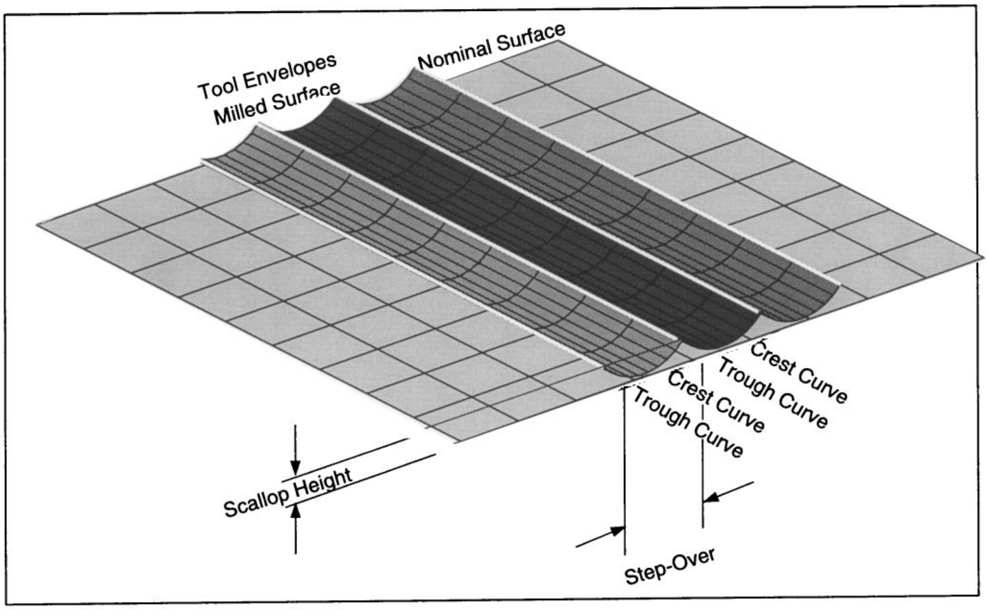

Fig. 1. Illustration of scallop height and step-over.

ized in the previous section. For a survey of different types of NC grinding machines please refer to Lilly *et al.* [4]. A detailed discussion on the process models for grinding can be found in Malkin [3]. In this section, the emphasis will be on parts of manufacturing data generation relevant for the motivation of this paper.

Much like the milling process, the manufacturing data for grinding consist of *process data* and *geometric data*. The process data required by the grinding machine are the feedrates, speeds and depths of cut. The feedrate is the rate of movement of the grinding tool along the grinding tool path. The speed is the rate of rotation of the grinding wheel about its own axis. The depth of cut for grinding operations is very small compared to that in milling operations and is generally lower than the maximum scallop height (height of the cusps or scallops as indicated in Fig. 1) on the milled part.

The geometric data are specified to the grinding (milling) machine through grinding tool paths by specification of cutter location (CL) points. The process of calculating the

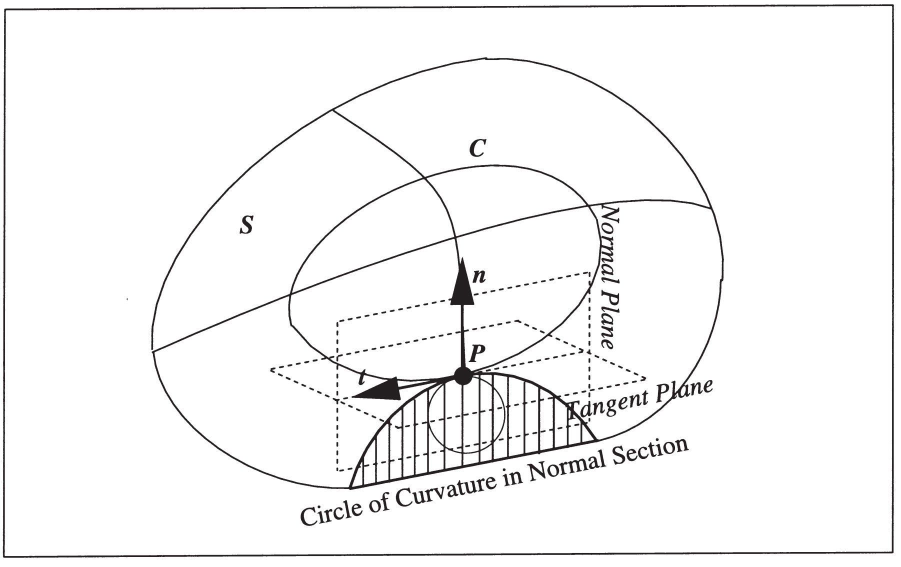

Fig. 2. Illustration of the circle of normal curvature.

CL points for grinding (milling) is referred to as grinding (milling) tool path generation. The spacing between tool paths depends on the geometry and type of grinding wheel being used. A search of literature revealed that iso-parametric curves on the milled part are used as grinding tool paths [7].

Of relevance is the literature on tool path generation for milling. Unlike for grinding, the literature in tool path generation for milling is abundant. Planar section curves [8], iso-parametric curves [9], projection curves [23] and offset curves [10, 21, 22] are used as tool paths for milling.

A major focus of the techniques for milling tool path generation has been to decrease the work done in grinding by reducing the scallops left by the milling tool. For example, the host of techniques for tool path generation by using offset curves [10–13] on the nominal surface, concentrate on achieving a user specified scallop height. One of the reasons for developing such techniques is to achieve a uniform depth of cut for grinding. Another technique to reduce the scallops involves using different geometries of milling tools and determining the placement and orientation of the tools to maximize the spacing between the tool paths for a given scallop height [14, 15]. You and Ehmann [16] have proposed a technique by which the milling tool is eccentrically mounted to remove the scallops. While the above techniques are able to reduce the scallops of the milled surface, there is still a need for further finishing the milled surface that is addressed in this paper.

The milled part is cusped due to the marks left by the milling tool as illustrated in Fig. 1. The cusps or scallops left behind by the milling tool need to be removed by grinding operations. Due to the tight tolerances on the nominal surface, it becomes mandatory that NC grinding is used in favor of manual grinding operations. For the same reason, it is also required that the die or mold (or the respective electrodes) are ground down to the final finish [17]. Currently, vision-based techniques, where the milled part is dyed a particular color, are used to detect when enough material has been removed by grinding [5]. The iterative use of surface inspection, surface fitting and grinding has been proposed to determine the depth of cut for grinding the milled part [7].

From the above literature it is observed that the control of the depth of cut for grinding is a very difficult task, due to the lack of information of the location and magnitude of the scallops on the milled part. While Duffie and Feng [7] estimate the grinding depth of cut by repeated measurement, surface fitting and surface localization, there is still a need for a method for manufacturing data generation that gives the user direct control over the depth of cut in grinding. In this paper, a new technique for grinding tool path generation is proposed that addresses the issues raised above.

The rest of this paper is structured as follows. Section 2 describes the representation and calculation of curves on the nominal surface. Specifically, Section 2.1 discusses the representation of curves and surfaces, and Section 2.2 discusses the calculation of geometric data for grinding tool paths that is enabled by the representation scheme. The method for generating the grinding tool paths is outlined in Section 3. In milling and grinding, an important concern is maintaining the surface roughness of the manufactured surface. Section 4 describes analytical methods for estimating the surface roughness. We conclude by presenting some results and summarizing in Section 5.

2. REPRESENTATION AND CALCULATION OF CURVES

In this section, we discuss the representation of curves and surfaces. Of interest, is the conceptually simple representation of curves on the nominal surface which provides a basis for integrating the geometric data generation for finishing operations (milling and grinding). In addition, the representation provides a starting point for geometric data generation for post milling operations, which was not available earlier.

2.1. *Representation of curves on the nominal surface*

The nominal surface is assumed to be a single, finite parametric surface $\boldsymbol{S}{:}\boldsymbol{r} = \boldsymbol{r}(u,v)$ with unique normals $\hat{\boldsymbol{n}} = \hat{\boldsymbol{n}}(u,v)$ defined at all points of $\boldsymbol{S}$. The milled surface (shown in Fig. 1) is bounded by the crest curves and trough curves. Hence, the milled surface is represented by the nominal surface and supplemented by information of the crest curves and trough curves (this can be extended to the ground surface as well). Such a representation of the manufactured surface, which was traditionally derived using measurement-based techniques, is useful in developing an integrated approach for manufacturing data generation, as will be shown in Section 3. In addition, such a representation of the manufactured surface helps in integrating the manufacturing and measurement, as will be shown in Section 4.

Curves defined with respect to the nominal surface are represented as curves in the parametric domain of $\boldsymbol{S}$. In addition, such curves are associated with a distance function from $\boldsymbol{S}$. Any curve $\boldsymbol{C}$ defined with respect to $\boldsymbol{S}$ is represented by the triple $\{u(t), v(t), h(t)\}$ and evaluated as shown in Eqn (1). The functions $u(t)$ and $v(t)$ represent a parametric curve, and the function $h(t)$ represents a distance function from $\boldsymbol{S}$. For example, the trough curves shown in Fig. 1, for a milled surface, lie on the nominal surface. Hence, for the trough curves of a milled surface, the function $h(t)$ is identically zero for all values of the parameter t.

$$\boldsymbol{c}(t) = \boldsymbol{r}[u(t),v(t)] + \hat{\boldsymbol{n}}[u(t),v(t)] \tag{1}$$

The tangent of the above curve can be obtained by differentiating Eqn (1) with respect to the parameter t as shown in Eqn (2). In this paper, it is assumed that bold faced letters symbolically represent vectorial quantities and ordinary letters scalar quantities. Carets $\hat{()}$ on the bold faced letters represent unit vectors. The first subscript of a symbol will imply partial differentiation with respect to the subscripted variable. A second subscript, if any, will represent evaluation of the symbol at a specific parameter value identified by the subscript. Where there is no ambiguity the dependance on the parameter will not be shown.

$$\boldsymbol{c}^t(t) = \frac{\boldsymbol{r}_u u_t + \boldsymbol{r}_v v_t + h_t \hat{\boldsymbol{n}} + h\hat{\boldsymbol{n}}_u u_t + h\hat{\boldsymbol{n}}_v v_t}{|\boldsymbol{r}_u u_t + \boldsymbol{r}_v v_t + h_t \hat{\boldsymbol{n}} + h\hat{\boldsymbol{n}}_u u_t + h\hat{\boldsymbol{n}}_v v_t|} \tag{2}$$

2.2. *Calculating curves on the nominal surface*

The technique for generating grinding tool paths involves tracking the crest curves at which maximum material is left behind. That is enabled by the representation described in the previous section. Hence, the method for generating grinding tool paths closely conforms with the method for generating milling tool paths. One of the steps in generating the tool paths involves determining the step-over. We define the step-over as the distance between corresponding points on adjacent trough/crest curves. For example, Fig. 1 illustrates the step-over between adjacent trough curves. Our method involves calculating the step-over from (a) the crest curve to the trough curve and (b) the trough curve to the crest curve. The step-over is calculated using the geometry of the milling tool. While calculating the step-over is necessary for milling tool path generation, calculating the scallop heights along the crest curves is also necessary to be able to accurately specify the depth of cut for grinding. Our method for calculating the step-over also takes into account the scallop height along the crest curves.

Of relevance in the step-over calculation is the shape of the tool (milling and grinding) in the vicinity of the nominal surface. First, the tool is replaced by a sphere of the same radius. This simplifies the computation of the swept section of the tool necessary in the step-over calculations. The swept sections (i.e., cross-sections of the tool swept volume) are circles that lie in the normal plane (i.e., plane spanned by the tangent and normal of the tool path at any given point) of the nominal surface. Second, at any point, the nominal surface is represented by its circle of normal curvature (of radius $\frac{1}{\kappa_n}$). The circle of normal curvature represents the radius of curvature at a given point, along a given direction in the tangent plane of the nominal surface. This is illustrated in Fig. 2.

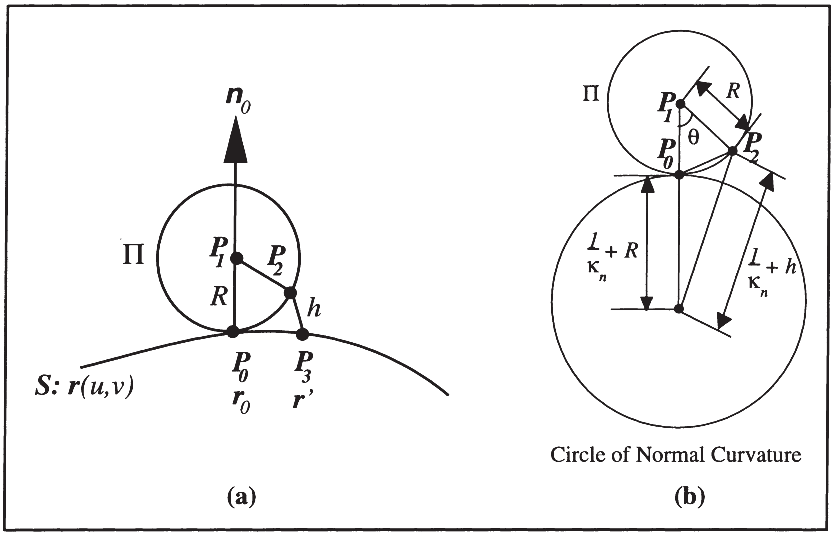

Fig. 3. Illustration of step-over from trough curve to crest curve.

2.2.1. *Trough curve to crest curve*. On a nominal surface $\boldsymbol{S}$, consider a point $\boldsymbol{P}_0$. This point $\boldsymbol{P}_0$ lies on a tool path $\boldsymbol{C}_1$ which is represented by the triple $\{u(t),v(t),0\}$. The use of a ball ended milling tool of radius R is assumed. The scallop height left behind by the milling tool is assumed to be h. From geometry, we know that the swept section of the milling tool (which is a circle of radius R) lies in the normal plane Π of the tool center path at $\boldsymbol{P}_1$, as shown in Fig. 3(a). Note that $\boldsymbol{P}_2$ which is a point on the crest curve, lies in Π. However, $\boldsymbol{P}_3$, the projection of $\boldsymbol{P}_2$ on $\boldsymbol{S}$, in general will not lie in Π. In Fig. 3(a) the scallop height h is the distance between $\boldsymbol{P}_2$ and $\boldsymbol{P}_3$. With this background, the expressions for $\boldsymbol{P}_0$, $\boldsymbol{P}_1$, $\boldsymbol{P}_2$ and $\boldsymbol{P}_3$ are generated in terms of R, h and the surface derivatives.

Below, the expressions for the points $\boldsymbol{P}_0$ and $\boldsymbol{P}_2$ are listed. The expression for $\boldsymbol{P}_2$ stems from the fact that the desired scallop height at $\boldsymbol{P}_2$ is h and hence $\boldsymbol{P}_2$ is offset from $\boldsymbol{S}$ at a distance of h. The subscript "0" is used to denote evaluation at the parameter t_0. The point $\boldsymbol{P}_2$ is expressed as a Taylor series expansion about $\boldsymbol{P}_0$.

$$\boldsymbol{P}_0 = \boldsymbol{r}(u_0,v_0) = \boldsymbol{r}_0 \tag{3}$$

$$\boldsymbol{P}_2 = \boldsymbol{r}_0 + h\hat{\boldsymbol{n}}_0 + \boldsymbol{r}_{u0}\delta u + h\hat{\boldsymbol{n}}_{u0}\delta u + \boldsymbol{r}_{v0}\delta v + h\hat{\boldsymbol{n}}_{v0}\delta v \tag{4}$$

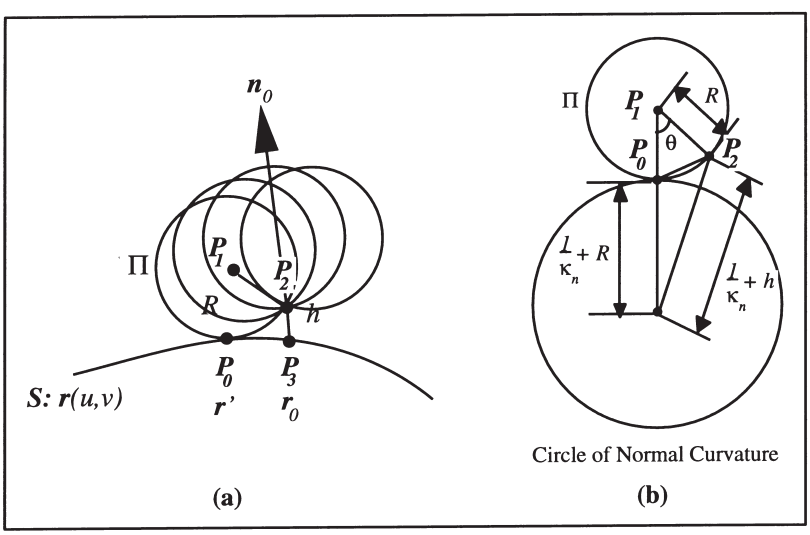

Fig. 4. Illustration of step-over from crest curve to trough curve.

There are two constraints to be enforced to calculate $\boldsymbol{P}_2$, (a) $\boldsymbol{P}_2$ must lie in the plane Π, and (b) $\boldsymbol{P}_2$ must be at a given distance d from $\boldsymbol{P}_0$. The constraints are shown in the equations below, where $\boldsymbol{c}_1^{\mathbf{t}}$ is the tangent to the tool center path which is also the normal of Π.

$$(\boldsymbol{P}_2 - \boldsymbol{P}_0)\cdot\boldsymbol{c}_1^t = 0 = \tag{5}$$
$$(\mathbf{r}_{u0}\mathrm{u}_t + \mathbf{r}_{v0}\mathrm{v}_t + \mathrm{R}\hat{\mathbf{n}}_{u0}\mathrm{u}_t + \mathrm{R}\hat{\mathbf{n}}_{v0}\mathrm{v}_t)\cdot(\mathbf{r}_{u0}\delta\mathrm{u} + \mathrm{h}\hat{\mathbf{n}}_{u0}\delta\mathrm{u} + \mathbf{r}_{v0}\delta\mathrm{v} + \mathrm{h}\hat{\mathbf{n}}_{v0}\delta\mathrm{v} + \mathrm{h}\hat{\mathbf{n}}_0)$$

$$\left|\boldsymbol{P}_2 - \boldsymbol{P}_0\right| = d = \left|h\hat{\boldsymbol{n}}_0 + \boldsymbol{r}_{u0}\delta u + h\hat{\boldsymbol{n}}_{u0}\delta u + \boldsymbol{r}_{v0}\delta v + h\hat{\boldsymbol{n}}_{v0}\delta v\right| \tag{6}$$

Figure 4(b) shows a picture illustrating the calculation of the quantity d. The normal section of the nominal surface is approximated by a circle of curvature. The angle θ is calculated by using the cosine rule as shown below. This approximation gives good results when the angle θ is small (less than 20 degrees).

$$\cos(\theta) = \frac{((1 + R\kappa_\mathrm{n})^2 + (R\kappa_\mathrm{n})^2 - (1 + h\kappa_\mathrm{n})^2)}{2R\kappa_\mathrm{n}(1 + R\kappa_\mathrm{n})} \tag{7}$$
$$\text{or}\ \cos(\theta) = \frac{R - h}{R}\ \text{if}\ \kappa_\mathrm{n} = 0$$

$$d = 2R\sin\left(\frac{\theta}{2}\right) \tag{8}$$

Using the notation from the Appendix, Eqn (5) can be simplified to yield a relation between δu and δv as follows.

$$-\frac{\delta u}{(fu_{t0} + gv_{t0} + hmu_{t0} + hnv_{t0} + Rmu_{t0} + Rnv_{t0} + hRqu_{t0} + hRpv_{t0})}$$
$$= \frac{\delta u}{U} = \frac{\Delta v}{V} = \lambda \tag{9}$$
$$= \frac{\delta v}{(eu_{t0} + fv_{t0} + hlu_{t0} + hmv_{t0} + Rlu_{t0} + Rmv_{t0} + hRou_{t0} + hRqv_{t0})}$$

Likewise, using the notation from the Appendix, Eqn (6) can be simplified to yield the following:

$$(e\delta u^2 + 2f\delta u\delta v + g\delta v^2) + 2h(l\delta u^2 + 2m\delta u\delta v + n\delta v^2) + h^2(o\delta u^2 + 2q\delta u\delta v + p\delta v^2) \tag{10}$$
$$= d^2 - h^2 = \mathbf{I} + 2h\mathbf{II} + h^2\mathbf{III}$$

where I, II and III represent the first, second and third fundamental forms of the surface $\boldsymbol{S}$, all evaluated at the parameter $t = t_0$.

The following expression from [18] is used to simplify Eqn (10).

$$\kappa_1\kappa_2\mathbf{I} - (\kappa_1 + \kappa_2)\mathbf{II} + \mathbf{III} = 0 \tag{11}$$

where κ_1 and κ_2 are the principal curvatures of the surface. II is expressed in terms of I by the following:

$$\mathbf{II} = \kappa_\mathrm{n}\mathbf{I} \tag{12}$$

where κ_n is the normal curvature of the nominal surface in the direction defined by δu and δv. Eqn (10) is simplified to the following:

$$\mathbf{I}(1 + 2h\kappa_n - h^2\kappa_1\kappa_2 + h^2\kappa_1\kappa_n + h^2\kappa_2\kappa_n) = 2Rh - h^2 \tag{13}$$

Eqn (9) is substituted into Eqn (13) and the resulting expression for λ is as follows:

$$\lambda = \pm\sqrt{\frac{d^2 - h^2}{(eU^2 + gV^2 + 2fUV)(1 + 2h\kappa_n - h^2\kappa_1\kappa_2 + h^2\kappa_1\kappa_n + h^2\kappa_2\kappa_n)}} \tag{14}$$

Given $\boldsymbol{P}_0$ (a point on the trough curve), using the above expressions, the point $\boldsymbol{P}_2$ (a point on the adjacent crest curve) and point $\boldsymbol{P}_3$ (the projection of $\boldsymbol{P}_2$ on $\boldsymbol{S}$) can be calculated. By considering all points on a given trough curve and a scallop height function $h(t)$, we can generate the entire crest curve as shown in Eqn (15). Note that the sign of λ determines whether the crest curve is to the left or right of $\boldsymbol{C}_1$.

$$u'(t) = u(t) + \lambda(t)U(t) \; v'(t) = v(t) + \lambda(t)V(t) \tag{15}$$

2.2.2. *Crest curve to trough curve*. Consider a point $\boldsymbol{P}_2$ on the nominal surface $\boldsymbol{S}$, which lies at a parameter t_0 on a crest curve $\boldsymbol{C}_2$ represented by the triple $\{u(t),v(t),h(t)\}$. Once again, the use of a ball ended milling tool of radius R is assumed. The scallop height at the parameter t_0 is assumed to be of a value h. From geometry it is known that the swept section (which is a circle of radius R) lies in the normal plane Π of the tool center path at $\boldsymbol{P}_1$, as shown in Fig. 5(a). In this case, the points on the crest curve are known and points on the trough curve need to be determined, such that the swept section is in contact with the nominal surface. The expressions for $\boldsymbol{P}_0$ and $\boldsymbol{P}_2$ are as follows:

$$\boldsymbol{P}_0 = \boldsymbol{r}_0 + \boldsymbol{r}_{u0}\delta u + \boldsymbol{r}_{v0}\delta v \tag{16}$$

$$\boldsymbol{P}_2 = \boldsymbol{r}_0 + h\hat{\boldsymbol{n}}_0 \tag{17}$$

There are two constraints to be enforced to calculate the point $\boldsymbol{P}_0$, (a) $\boldsymbol{P}_2$ must lie in the plane Π, and (b) $\boldsymbol{P}_2$ must be at a distance d from $\boldsymbol{P}_0$, where expressions for obtaining d are shown in Eqn (7) and (8). The constraints are shown in the equations below where $\boldsymbol{c}_2^{\mathbf{t}}$ is the tangent to the crest curve, which is also the normal to the line from $\boldsymbol{P}_1$ to $\boldsymbol{P}_2$.

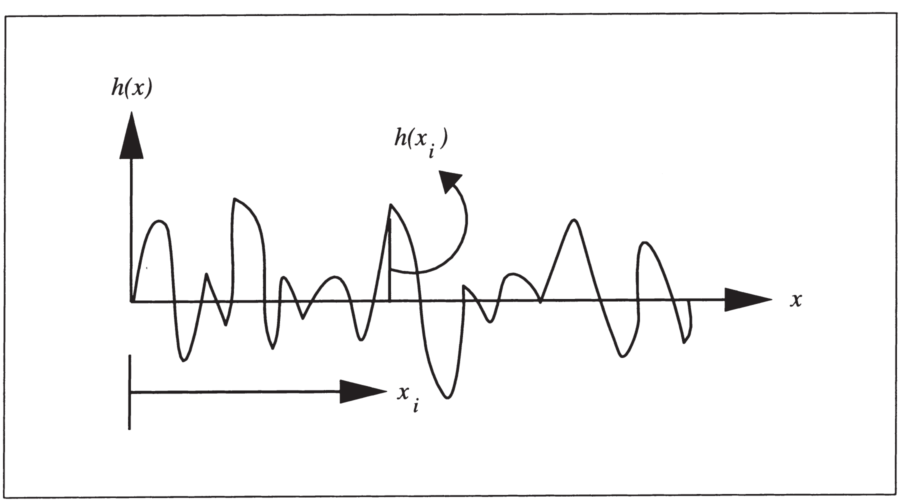

Fig. 5. Illustration of manufactured part profile.

$$(\boldsymbol{P}_2 - \boldsymbol{P}_0)\cdot\boldsymbol{c}_2^t = 0 = \tag{18}$$
$$(\boldsymbol{r}_{u0}u_t + \boldsymbol{r}_{v0}v_t + h\hat{\boldsymbol{n}}_{u0}u_t + h\hat{\boldsymbol{n}}_{v0}v_t + h_t\hat{\boldsymbol{n}}_0)\cdot(\boldsymbol{r}_{u0}\delta u + \boldsymbol{r}_{v0}\delta v - h\boldsymbol{n}_0)$$

$$|\boldsymbol{P}_2 - \boldsymbol{P}_0| = d = |-h\hat{\boldsymbol{n}}_0 + \boldsymbol{r}_{u0}\delta u + \boldsymbol{r}_{v0}\delta v| \tag{19}$$

We simplify Eqn (18) using the notation from the Appendix to yield:

$$\delta u(eu_t + fv_t + hlu_t + hmv_t + Rlu_t + Rmv_t + hRou_t + hRqv_t) + \tag{20}$$
$$\delta v(fu_t + gv_t + hmu_t + hnv_t + Rmu_t + Rnv_t + hRqu_t + hRpv_t) = (R - h)h_t$$

We re-write in the same form as Eqn (9) by taking into account the fact that the term $(R - h)h_t$ is several orders of magnitude smaller than the other coefficients U and V. The reason is that the variation in the scallop height along the tool paths is very small. Simplification will show that the coefficients U and V have the same expressions as in Eqn (9) as follows.

$$\frac{\delta u}{U} = \frac{\delta v}{V} = \lambda \tag{21}$$

Using the same procedure as in the previous section, Eqn (19) simplifies to the following:

$$\mathbf{I} = d^2 - h^2 \tag{22}$$

Solving Eqn (21) and (22), and adopting the notation from the Appendix, we have the following expression for λ:

$$\lambda = \pm\sqrt{\frac{d^2 - h^2}{(eU^2 + gV^2 + 2fUV)}} \tag{23}$$

Given the crest curve $\boldsymbol{C}_2$, the trough curve can be obtained for all values of t, as shown in Eqn (24). Once again, the sign of λ determines whether the trough curve which is generated lies to the left or right of $\boldsymbol{C}_2$.

$$u'(t) = u(t) + \lambda(t)U(t) \quad v'(t) = v(t) + \lambda(t)V(t) \tag{24}$$

3. TOOL PATH GENERATION

In this section, a novel technique for grinding tool path generation is outlined. This technique is based on tracking the crest curves of the milled surface, in order to maximize material removal where it is needed most. Since the milling tool paths determine the location and magnitude of the scallop height on the milled surface, our technique for grinding tool path generation is coupled with the milling tool path generation in Sarma and Dutta [10]. In this paper, we do not consider the tool orientation problem, which is a part of our ongoing work. However, note that determining the tool orientation is necessary for generating sufficient surface speeds for grinding.

The method for milling tool path generation [10] involves using *scallop height functions* for manipulating the local and global geometry of the milling tool paths to give the user control over practical metrics such as length, curvature and number of tool paths. Such metrics, which give the user valuable information related to productivity (time and accuracy of machining), are not currently available in commercial CAD/CAM systems. One example of a scallop height function is the constant scallop height function, for which the scallop height is a constant along the crest curve. For further details of scallop height functions and different types of scallop height functions, please refer to Sarma and Dutta [10].

The input and procedure for grinding tool path generation is as follows:

***Input*:**

1. Nominal surface $\boldsymbol{S}$**:**$\boldsymbol{r}(u,v)$ and its parametric bounds.
2. Milling and grinding part orientations.
3. Milling and grinding tool radii.
4. Starting curve $\boldsymbol{C}_0$ (crest curve or trough curve).
5. Maximum and minimum values of scallop height.
6. Type of scallop height function to be used.

***Procedure*:**

1. Calculate the scallop height function $h(t)$ based on the local properties of the nominal surface along the given starting curve $\boldsymbol{C}_0$.
2. Using the step-over calculation in Section 3, compute $\boldsymbol{C}_1$ from $\boldsymbol{C}_0$. If $\boldsymbol{C}_0$ is a crest curve (trough curve) then $\boldsymbol{C}_1$ is a trough curve (crest curve).
3. If $\boldsymbol{C}_1$ lies within the parametric bounds of $\boldsymbol{S}$, then $\boldsymbol{C}_0 \leftarrow \boldsymbol{C}_1$ and proceed to Step 1. If $\boldsymbol{C}_1$ lies outside the parametric bounds of $\boldsymbol{S}$, then the tool paths span $\boldsymbol{S}$ and tool path generation is complete.
4. The trough curves are used as milling tool paths and the crest curves are used as grinding tool paths. The scallop height functions along the crest curves are used to determine the depth of cut for grinding.

4. ESTIMATES OF SURFACE ROUGHNESS

The surface roughness [19] on the manufactured surface results from the marks left by the cutting tool. The surface roughness is usually of concern in the manufacture of dies and molds, since it affects the functionality. While in tool path generation the user specifies the scallop height, it is the surface roughness that is of interest to the user for determining the functional characteristics of the manufactured surface.

In this section, we outline a procedure to analytically estimate the surface roughness of the milled and ground surfaces. The analytical estimates of surface roughness would not have been possible without the representation of the milled and ground surfaces. The analytical estimates provide a starting point for the measurement or inspection operations which are very data intensive and often times expensive for free-form surfaces.

Surface roughness is measured in terms of surface roughness parameters that might be amplitude based, spacing based or hybrid. Amplitude parameters reflect the variations in the amplitude of the profile. Spacing parameters reflect the wavelength of the manufactured part profile. Hybrid parameters attempt to take into account the amplitude and wavelengths of the manufactured part.

The most commonly used surface roughness parameters are amplitude parameters such as the average roughness (R_a), the maximum peak to valley roughness (R_t) and the root mean square roughness (R_q). Surface roughness parameters give an estimate of performance related characteristics of the manufactured part, such as reflectivity, aesthetics, lubricant retention, wear characteristics, etc. By themselves, the surface roughness parameters cannot be used to determine the functional characteristics of the manufactured surface [12, 20]. The functional characteristics of the manufactured surface are better determined by studying the total part profile. This is one of the advantages for having a representation of the manufactured surface in terms of the trough curves and crest curves. The expressions for calculating the roughness values are:

$$R_a = \int_0^l h(x)\mathrm{d}x \tag{25}$$

$$R_t = max\,|h(x)| + \ min\,|h(x)| \tag{26}$$

$$R_q = \int_0^l [h(x)]^2 \mathrm{d}x \tag{27}$$

In the above equations, it is assumed that $h(x)$ is a function that represents the manufactured part profile as measured from a reference mean line as shown in Fig. 5, l represents the length of the profile being assessed or a sampling length.

4.1. *Surface roughness after milling*

Consider a given sample length l over which the surface roughness parameters are being evaluated. Note that though the sampling length in its traditional usage* is l, the integrations as shown in Eqn (25)–(27) need to be performed over the arc length L of the curve C, as will be seen later in this section. The sampling length and direction are specified by a plane P intersecting the milled part as shown in Fig. 6. Consider the curve of intersection C of the plane P and the designed part. Also, consider the points of intersection of the crest curves (S_i) with P and the points of intersection of the trough curves (T_i) with the plane P as illustrated in Fig. 7(a). The points S_i are assumed to be at distances h_i from the nominal surface and this information is directly obtained from the representation of the milled surface. As shown in Fig. 7(a), we assume that the milled part profile is suitably approximated by circular arcs obtained by fitting arcs through consecutive points S_i, T_i and $S_i + 1$.

The height function $h(x)$, as shown in Fig. 7(b), is derived by considering: (a) the circles of normal curvature at the points T_i; and (b) the distances h_i of the points S_i from the nominal surface as given by the crest curves. This is illustrated in Fig. 8. The equation for $h(x)$, obtained by applying the cosine rule, is given as follows:

$$h(x) = \frac{2R_i r_i}{2(R_i + r_i)\cos\theta_i - 2R_i} - R_i - \theta_{imin} \leq \theta_i \leq \theta_{imax} \tag{28}$$

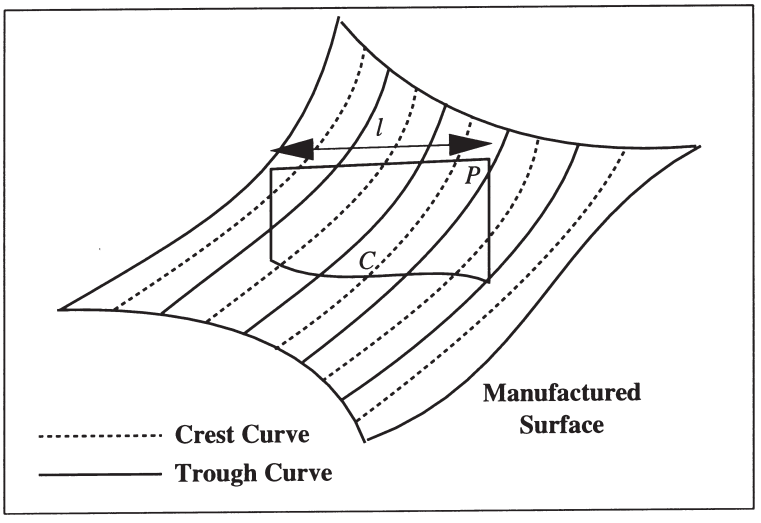

Fig. 6. Illustration of sampling length and direction specification.

*For traditional surface roughness measuring equipment, the sampling length is specified in terms of a straight line motion of the stylus or measuring head. In the case of measuring flat parts, this is directly, the length over which the surface roughness is measured. For free form surfaces it is still convenient to specify the motion of the stylus in terms of object domain lengths, however for evaluating the surface roughness, the arc length of the curve has to be used.

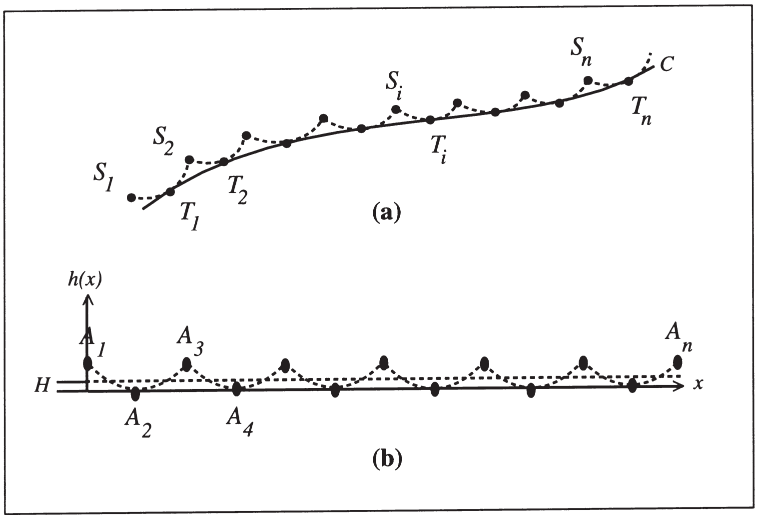

Fig. 7. Illustration of surface roughness along sampling length.

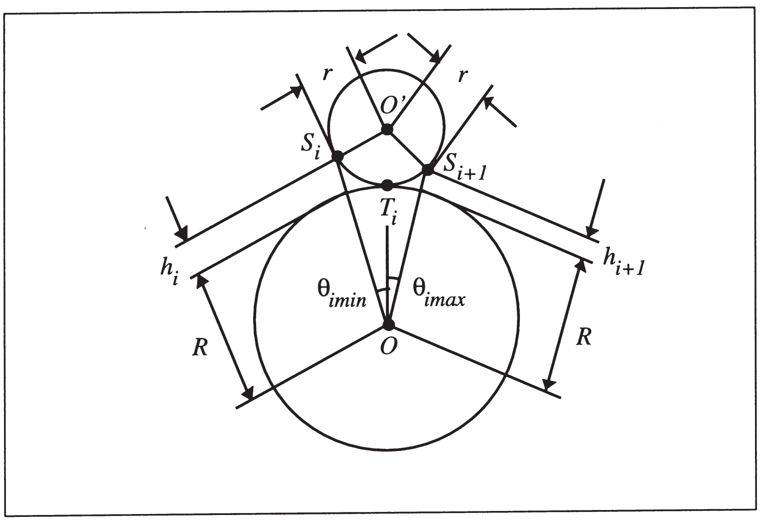

Fig. 8. Derivation of the height function.

$$x = \sum_{j=1}^{i-1} R_j(\theta_{jmax} + \theta_{jmin}) + R_i\theta_i \tag{29}$$

Note that the function $h(x)$ is given in terms of the angle θ, which is related to the variable x through Eqn (29). This conversion of variables is necessary since x, which is the arc length along the sampling length, is the variable in the integrations as shown in Eqns (25)–(27).

In Eqns (28) and (29), $\theta_{i\min}$ and $\theta_{i\max}$ are the angles $\angle O_i'O_iS_i$ and $\angle O_i'O_iS_{i+1}$, respectively, and can be calculated using the cosine rule as follows:

$$\cos\theta_{imin} = \frac{(R_i + r_i)^2 + (R_i + h_i)^2 - r_i^2}{2(R_i + r_i)(R_i + h_i)} \tag{30}$$

$$\cos\theta_{imin} = \frac{(R_i + r_i)^2 + (R_i + h_{i+1})^2 - r_i^2}{2(R_i + r_i)(R_i + h_{i+1})} \tag{31}$$

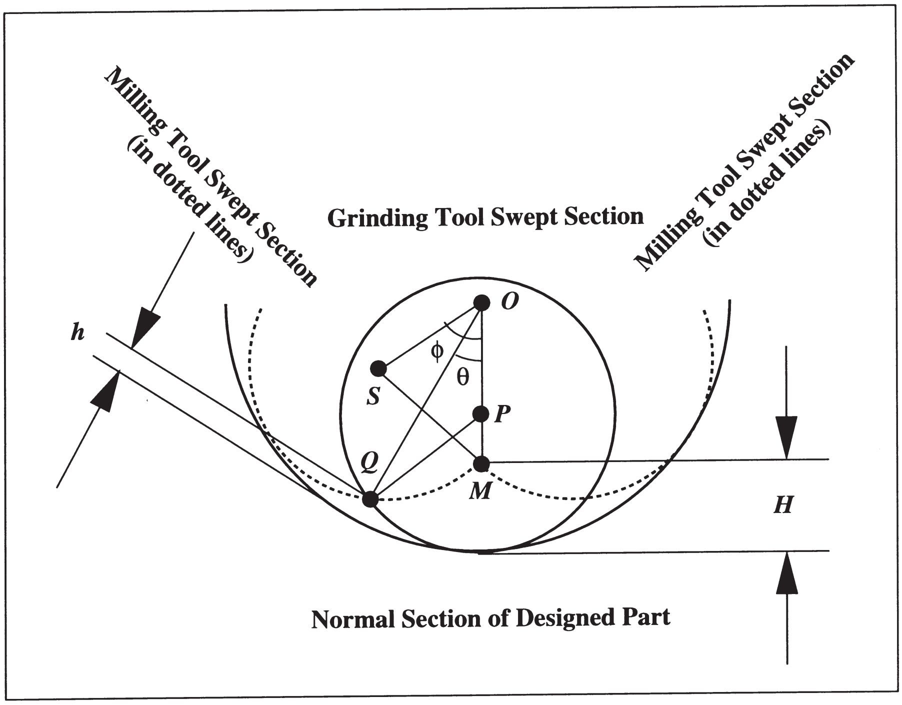

Fig. 9. Illustration of milling and grinding scallop heights.

As mentioned earlier, though the sampling length is l, the evaluation length or the length over which the surface roughness is evaluated is L, where L is given by:

$$L = \sum_{i=1}^{n} R_i(\theta_{imax} + \theta_{imin}) \tag{32}$$

Before we are able to evaluate the surface roughness parameters, the mean line has to be estimated. This can be estimated by considering the height function [Fig. 7(b)] and evaluating the mean line, such that the sum of areas A_1,A_3,..., is equal to the sum of areas A_2,A_4,.... We can solve for the mean line using the following equation:

$$H = \frac{1}{l}\int_0^L h(x)\mathrm{d}x \tag{33}$$

The roughness parameters can now be estimated as follows:

$$R_a = \int_0^L |h(x) - H|\mathrm{d}x \tag{34}$$

$$R_t = |\,max(h_i - H)| + |\,min(h_i - H)| \tag{35}$$

$$R_q = \int_0^L [h(x) - H]^2\mathrm{d}x \tag{36}$$

All the above equations can be evaluated using numerical integration rules, e.g., trapezoidal rule, Simpson's rule, etc.

4.2. *Grinding tool specifications*

In this section, we outline a technique for estimating the radius of the grinding tool and the grit size of abrasive particles of the grinding tool based on the scallop heights.

4.2.1. *Scallop height for non-convex parts*. If the nominal surface is non-convex, the largest radius of the grinding tool cannot exceed the radius of the milling tool in order to avoid gouging.* Hence, the radii of the grinding and milling tools are selected to be the same. In such a case, grinding yields specific values of the scallop height, and the maximum scallop height cannot be specified *a priori*. Figure 9 shows the milling scallop height (H) and the grinding scallop height (h) on a given normal section (radius R) of the nominal surface.

The radius (r) of the swept section of the grinding tool is the same as that of the swept section of the milling tool. The scallop height h can be calculated by considering the points O, P, Q, S and M, where O is the center of the normal section, P is the center of the grinding tool swept section, Q is a point on the ground cusp, S is the center of the milling tool swept section and M is a point on the milled cusp. From geometry, we know the lengths of the following sides: $\overline{OM} = R - h$, $\overline{OP} = R - r$, $\overline{PQ} = r$, $\overline{OQ} = R - h$, $\overline{OS} = R - r$ and $\overline{SM} = r$. *In addition, we also know that* $\theta = \phi/2$. *Now we write the expressions for the cosine rule for the two triangles OSM* and *OQP*, from which we will be able to calculate the ground scallop height h.

$$\cos\phi = \frac{(R - H)^2 + (R - r)^2 - r^2}{2(R - H)(R - r)} \tag{37}$$

$$\cos\theta = \frac{(R - h)^2 + (R - r)^2 - r^2}{2(R - h)(R - r)} \tag{38}$$

Note that if the scallop height on the ground surface is larger than desired, another pass of grinding might be needed. Theoretically, in such cases, the grinding crest curves could be used as grinding tool paths.

4.2.2. *Tool radius for convex parts*. If the nominal surface is convex, then there is no restriction on the radius of the grinding tool. Hence, we outline a procedure to calculate the radius of the grinding tool based on the desired scallop height h on the ground part. Fig. 10 shows the milling scallop height (H) and the grinding scallop height (h) on a given normal section (radius R) of the nominal surface. In this case, the radius (r) of the swept section of the grinding tool is different from the radius (s) of the swept section of the milling tool.

The grinding tool radius r can be calculated by considering the points O, P, Q, S and M, where O is the center of the normal section, P is the center of the grinding tool swept section, Q is a point on the ground cusp, S is the center of the milling tool swept section and M is a point on the milled cusp. From geometry, we know the lengths of the following sides: $\overline{OM} = R + h$, $\overline{OP} = R + r$, $\overline{PQ} = r$, $\overline{OQ} = R + h$, $\overline{OS} = R + s$ and $\overline{SM} = s$. In this case, we make the assumption that $\theta = \phi/2$. Now we write the expressions for the cosine rule for the two triangles *OSM* and *OQP*, from which we will be able to calculate the radius of the grinding tool r.

*Note that if the radius of the milling tool determined on the basis of gouging is too large for practical purposes, then a smaller milling tool may be used. In such a case, it is probable that a larger grinding tool could be utilized and the size of the grinding tool estimated based on the desired scallop heights on the ground part. The procedure then, will be similar to that for convex parts.

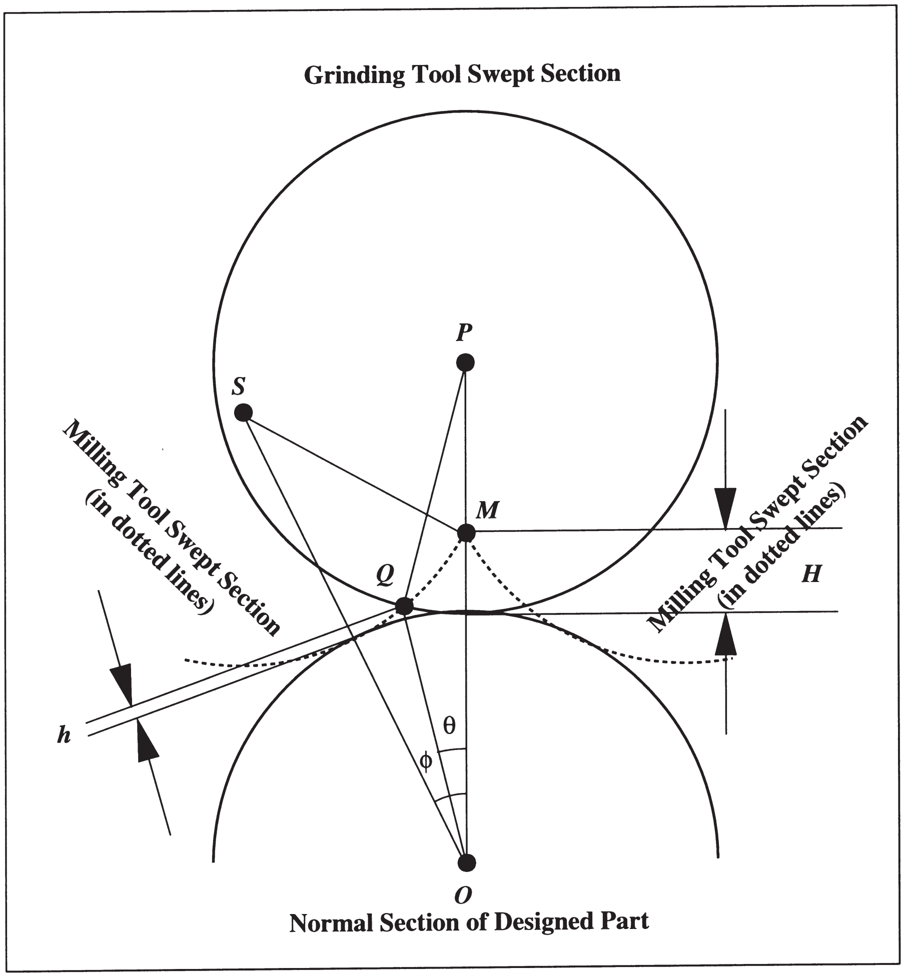

Fig. 10. Illustration of milling and grinding scallop heights.

$$\cos \phi = \frac{(R + H)^2 + (R + s)^2 - s^2}{2(R + H)(R + s)} \tag{39}$$

$$\cos \theta = \frac{(R + h)^2 + (R + r)^2 - r^2}{2(R + h)(R + r)} \tag{40}$$

Note that for both convex and non-convex parts, the actual scallop height will vary from the ideal scallop heights calculated in the above equations, due to the random topography of the grinding wheel surface, vibrations, thermal effects, etc. In this paper we only consider the geometric effects of the tools and ignore the physics of the machining process.

4.2.3. *Grit size determination*. While the tool radii determined in the previous subsections affect the scallop height or surface roughness across the lay, the grit size of the grinding wheel determines the surface roughness along the lay. The lay is the directionality of the tool marks on the manufactured part. Typically, the surface roughness across the lay is seven-eight times larger than the surface roughness along the lay [3]. Hence, the criterion for determining the grit size is to select the size of the abrasive particles lesser than the magnitude of the peak to valley roughness value (R_t), across the lay.

4.3. *Surface roughness after grinding*

The surface roughness after grinding can be determined by the method described in Section 4.1. In addition, there will be intermediate points which have to be introduced in the calculations, such as the points on the ground cusps Q (shown in Fig. 10).

5. RESULTS AND SUMMARY

Our method for generating tool paths has been implemented on the Silicon Graphics Personal Iris workstation in C + +. The ACIS geometric modeler has been used for generating tool paths. The user interface for our implementation uses the Tcl/Tk and GL libraries. Figure 11 shows a scaled model of an aeroplane engine housing which has been milled and ground using our method for tool path generation. The scaled model of the aeroplane engine housing has been first milled using a quarter inch milling tool for a constant scallop height of 0.005 inches (which is an R_a of 0.0025 inches). The front part of the engine housing shown in Fig. 11 shows the milled surface. Next, the back half of the engine housing shown in Fig. 11, is ground using a half inch grinding tool for a scallop height of 0.0025 inches (which is an R_a of 0.0013 inches). The close-ups of the milled and ground surfaces are shown in Fig. 12 for comparison, where the milled surface is on the left and the ground surface on the right.

Summarizing, a new technique for tool path generation for grinding was developed. This technique for tool path generation was enabled by the representation of the manufactured surface in terms of the crest curves and trough curves. In addition, the representation for tool path generation allowed us to develop analytical estimates of the surface roughness of the manufactured surface (milled and ground surfaces).

Our future work involves developing a general representation scheme for the manufactured surfaces. One use for manufactured surface representations (in tool path generation) has been demonstrated in this paper. The main advantage of manufactured surface representations is the seamless flow of information across the activities of design, manufacturing and measurement.

Acknowledgements—The financial support from AFOSR grant number F49620-95-1-0209 is gratefully acknowledged.

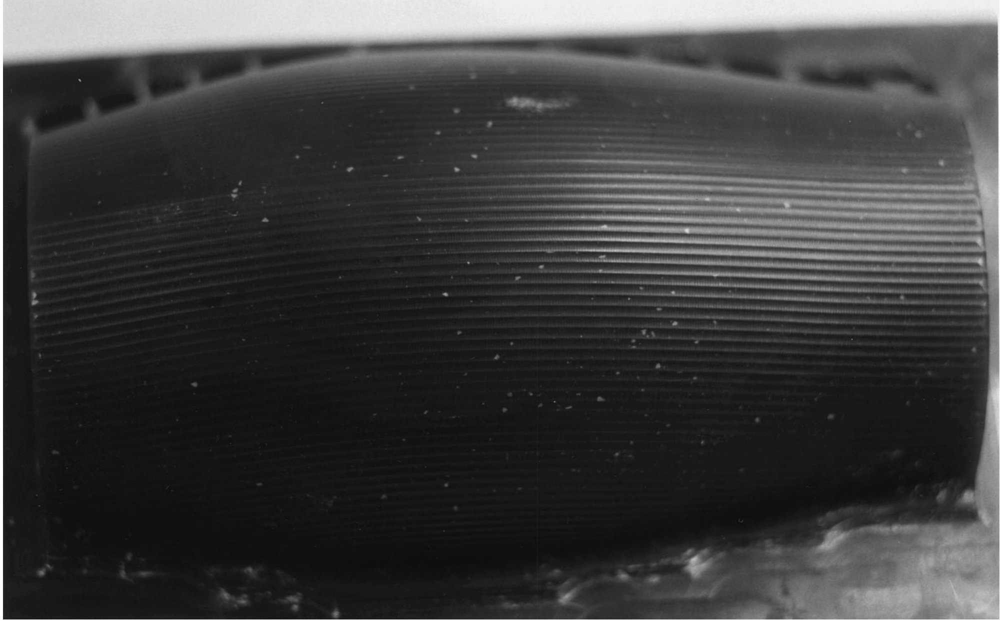

Fig. 11. Scaled model of an aeroplane engine housing.

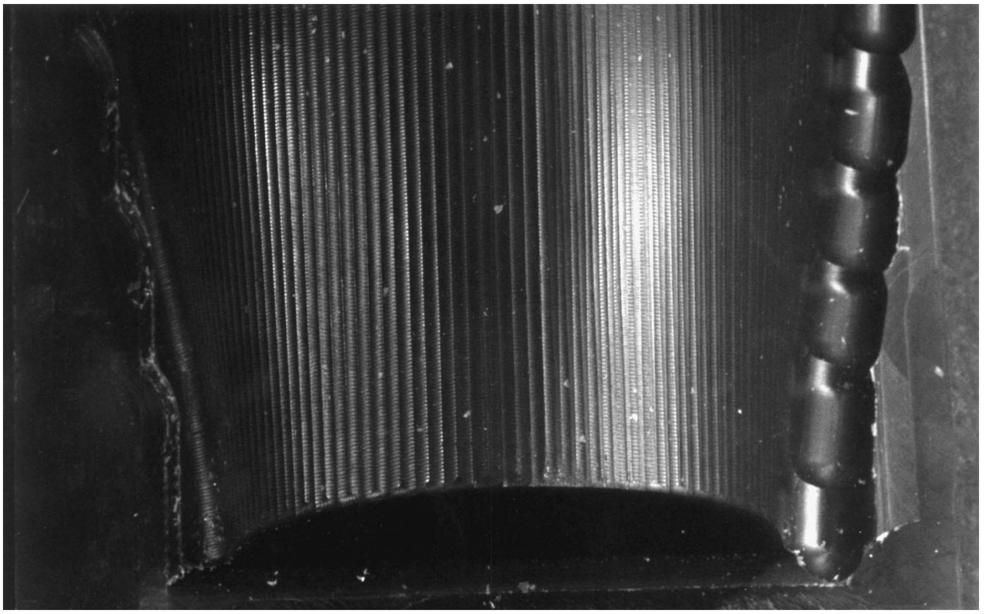

Fig. 12. Comparison of milled and ground surfaces.

REFERENCES

[1] Altan, T., Lilly, B. W., Kruth, J. P., Konig, W., Tonshoff, H. K., VanLuttervelt, C. A. and Khairy, A. B., Advanced techniques for die and mold manufacturing. *Annals of the CIRP*, 1993, **42**(2), 707–716.
[2] Lange, K., *Handbook of Metal Forming*, McGraw Hill, USA, 1985.
[3] Malkin, S., *Grinding Technology: Theory and Applications of Machining with Abrasives*, John Wiley, U.S.A., 1989.
[4] Lilly, B. W., Bailey, R. W. and Altan, T., Automated finishing of dies and molds: a state of the art review. *Computer Aided Design and Manufacture of Dies and Molds*, ASME, 1988. 1988.
[5] Whitney, D. E. and Tung, E. D., Robot grinding and finishing of cast iron stamping dies. *Transactions of the ASME*, 1992, **114**, 132–114.
[6] McMaster-Carr, McMaster-Carr Supply Company: Catalogue 99, 1993.
[7] Duffie, N. A. and Feng, S. C., Surface finishing with automated inspection and grinding. *Computer Aided Design and Manufacture of Dies and Molds*, ASME, 1988, 19–28.
[8] Huang, Y. and Oliver, J. H., Non-constant parameter NC tool path generation on sculptured surfaces. *International Journal of Advanced Manufacturing Technology*, 1994, **9**, 281–290.
[9] Loney, G. C. and Ozsoy, T. M., NC machining of free form surfaces. *Computer Aided Design*, 1987, **19**(2), 85–89.
[10] Sarma, R. and Dutta, D., The geometry and generation of NC tool paths. *ASME Journal of Mechanical Design*, 1997, **119**(2), 253–258.
[11] Mortensen, F. L., Constant scallop height tool paths for sculptured surfaces. Master Thesis, Brigham Young University, 1988.
[12] Tabenkin, A. N., The crowning importance of surface finish specs. *Machine Design*, 1984, 99–102.
[13] Lin, R. S. and Koren, Y., Efficient tool path planning for machining free-form surfaces. *Journal of Engineering for Industry*, **1996, 118**(1), 20–28.
[14] Jensen, C. G. and Anderson, D. C., Accurate tool placement and orientation for finish surface machining. *Concurrent Engineering, PED, ASME*, 1992, **59**, 127–145.
[15] Mullins, S. H., Jensen, C. G. and Anderson, D. C., Scallop elimination based on precise 5-axis tool placement, orientation and step-over calculations. *Proceedings of the 19th annual ASME Design Automation Conference*, Albuquerque, NM, Part 2, 1993.
[16] You, S. J. and Ehmann, K. F., Scallop removal in die milling by tertiary cutter motion. *Journal of Engineering for Industry*, 1989, **111**(3), 213–219.
[17] Beard, T., Machining in circles. *Modern Machine Shop*, 1996, **69**(2), 52–60.
[18] Struik, D. J., *Lectures on Classical Differential Geometry*, Dover Publications, U.S.A., 1950.
[19] Whitehouse, D. J., *Handbook of Surface Metrology*, IOP Publishing, Philadelphia, U.S.A., 1994.
[20] Koelsch, J. R., Troubleshooting finish problems. *Manufacturing Engineering*, 1994, **113**(3), 53–55.
[21] Chou, J. J. and Cohen, E., Constant scallop height tool path generation. Technical Report UUCS-89-0911, University of Utah, 1989.
[22] Suresh, K. and Yang, D. C. H., Constant scallop height machining of free form surfaces. *ASME Journal of Engineering for Industry*, 1994, **116**, 253–259.
[23] Unigraphics, EDS Unigraphics On-line Documentation, Version 12.0, 1993.

APPENDIX

:

Expressions for the partial derivatives of the unit surface normal given below are derived in this Appendix.

$$n = \frac{r_u \times r_v}{|r_u \times r_v|} \tag{A1}$$

Since the normal is orthogonal to any vectors in the tangent plane we have the following:

$$n \cdot r_u = n \cdot r_v = 0 \tag{A2}$$

Differentiating with respect to u and v we have:

$$n \cdot r_{uu} + n_u \cdot r_u = 0 \tag{A3}$$

$$n \cdot r_{vu} + n_v \cdot r_u = 0 \tag{A4}$$

$$n \cdot r_{uv} + n_u \cdot r_v = 0 \tag{A5}$$

$$n \cdot r_{vv} + n_v \cdot r_v = 0 \tag{A6}$$

Since $r_{uv} = r_{vu}$ we have:

$$n_u \cdot r_v = n_v \cdot r_u \tag{A7}$$

Now consider the first and second fundamental forms of the surface:

$$\mathbf{I} = \delta r \cdot \delta r = e\delta u^2 + 2f\delta u\delta v + g\delta v^2 \tag{A8}$$

$$\mathbf{II} = -\ n \cdot \delta r = l\delta u^2 + 2m\delta u\delta v + n\delta v^2 \tag{A9}$$

We define the scalars of the first and second fundamental forms of the surface, respectively:

$$e = r_u \cdot r_u \quad f = r_u \cdot r_v \quad g = r_v \cdot r \tag{A10}$$

$$l = -\ n \cdot r_{uu} \quad m = -\ n \cdot r_{uv} \quad n = -\ n \cdot r_{vv} \tag{A11}$$

Eqns (A2)–(A5) can be rewritten as:

$$n_u \cdot r_u = l \tag{A12}$$

$$n_u \cdot r_v = m \tag{A13}$$

$$n_v \cdot r_v = n \tag{A14}$$

We could also express (A12)–(A14) as follows:

$$\begin{bmatrix} n_u \\ n_v \end{bmatrix} \cdot \begin{bmatrix} r_u \\ r_v \end{bmatrix} = \begin{bmatrix} l & m \\ m & n \end{bmatrix} \tag{A15}$$

If we express the derivatives of the normals as:

$$\begin{bmatrix} n_u \\ n_v \end{bmatrix} = \begin{bmatrix} a & b \\ c & d \end{bmatrix} \begin{bmatrix} r_u \\ r_v \end{bmatrix} \tag{A16}$$

Then taking a dot product of the vector $[r_u, r_v]^T$ and $[n_u, n_v]^T$ we have:

$$\begin{bmatrix} n_u \\ n_v \end{bmatrix} \cdot \begin{bmatrix} r_u \\ r_v \end{bmatrix} = \begin{bmatrix} a & b \\ c & d \end{bmatrix} \begin{bmatrix} e & f \\ f & g \end{bmatrix} \tag{A17}$$

From Eqns (A15) and (A16) we can solve for the quantities a, b, c and d as:

$$\begin{bmatrix} a & b \\ c & d \end{bmatrix} = \frac{\begin{bmatrix} l & m \\ m & n \end{bmatrix}\begin{bmatrix} g & -f \\ -f & e \end{bmatrix}}{(eg - f^2)} \tag{A18}$$

To shorten the notation we have:

$$o = n_u \cdot n_u \quad q = n_u \cdot n_v \quad p = n_v \cdot n \tag{A19}$$

As an interesting note, there exists a third fundamental form of the surface [18] whose coefficients are given in Eqn (A19). It can be given as:

$$\mathbf{III} = \delta n \cdot \delta n = o\delta u^2 + 2q\delta u\delta v + p\delta v^2 \tag{A20}$$

The physical significance of the third fundamental form of the surface can be explained as the square of the differential arc length of the spherical image of the surface.